Plant Stress 19 (2026) 101223

Contents lists available at ScienceDirect

Plant Stress

journal homepage: www.sciencedirect.com/journal/plant-stress

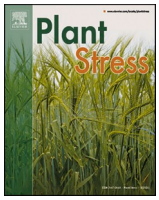

Exogenous nootkatone impairs nitrogen nutrition by promoting ammonium over nitrate uptake in *Arabidopsis thaliana*

Alice Zambelli [a,1], Michele Pesenti [a,1], Giorgio Lucchini [a], Adela María Sánchez-Moreiras [b,c], Luca Espen [a], Fabrizio Araniti [a,*], Fabio Francesco Nocito [a]

[a] Dipartimento di Scienze Agrarie e Ambientali – Produzione, Territorio, Agroenergia. Università degli Studi di Milano. Via Celoria 2, 20133 Milano, Italy
[b] Instituto de Agroecoloxía e Alimentación (IAA), Universidade de Vigo, Campus Auga, 32004 Ourense, Spain
[c] Departamento de Bioloxía Vexetal e Ciencias do Solo, Facultade de Bioloxía, Universidade de Vigo, Campus Lagoas-Marcosende s/n, 36310 Vigo, Spain

ARTICLE INFO

Keywords:
Allelochemical toxicity
Amino acids
Natural compounds
Metabolomic reprogramming
Stable nitrogen isotope analysis

ABSTRACT

Nootkatone, a natural sesquiterpenoid, has recently emerged as a candidate allelochemical for sustainable weed management. However, its phytotoxic effects and underlying mechanisms in plants remain poorly understood. In this study, we present a comprehensive characterization of nootkatone-induced toxicity in *Arabidopsis thaliana*, integrating physiological, metabolomic, and nutritional analyses. Exposure to increasing concentrations of nootkatone resulted in dose-dependent reductions in biomass and photosynthetic efficiency, accompanied by visible morphological damage. GC–MS-based metabolomic profiling revealed significant reprogramming of primary metabolism, particularly affecting amino acid biosynthesis and nitrogen-related pathways. Network analysis identified glutamic acid as an important metabolic hub, linking nitrogen assimilation to stress-related responses. Nutritional profiling and stable isotope analysis demonstrated that nootkatone disrupts nitrogen homeostasis by promoting ammonium uptake over nitrate assimilation. This shift was confirmed by ^{15}N-labeled experiments, which showed reduced nitrate uptake and compensatory ammonium absorption. The altered nitrogen source preference was associated with increased accumulation of ammonium, free amino acids, and nitrogen-rich intermediates, consistent with typical symptoms of ammonium toxicity. These findings suggest a potential mechanism underlying nootkatone-induced phytotoxicity and underscore its promise as a bioactive compound for sustainable and environmentally friendly weed management strategies.

Introduction

Weeds represent one of the major constraints affecting agricultural productivity globally, significantly reducing crop yields through competition for environmental resources, including mineral nutrients, water, light, and space (Chauhan, 2020). Traditional weed management strategies primarily rely on synthetic chemical herbicides, which – despite their effectiveness – have given rise to significant environmental and agronomic issues mainly linked to the contamination of water resources, their adverse effects on non-target species, and the troubling spread of herbicide-resistant weed biotypes (Powles and Yu, 2010; Duke and Heap, 2017; Westwood et al., 2018). Moreover, the increasing public concern regarding food safety, ecosystem sustainability, and biodiversity protection has propelled the search for more sustainable and eco-friendly weed control alternatives, thus redirecting research attention toward natural compounds and bioherbicides (Dayan and Duke, 2010; Duke et al., 2022). In such a context, allelopathy – the chemical interaction between plants mediated by secondary metabolites released into the environment – has garnered considerable scientific interest as a promising source of novel phytotoxic compounds for the development of bio-based herbicides (Satyanarayana Murthy et al., 2025).

Plants synthesize a diverse array of specialized metabolites, including phenolics, alkaloids, and terpenoids, which can significantly impact the growth, development, and survival of neighboring plant species (Butnariu and Koirala, 2025; Zambelli et al., 2025). These naturally derived compounds offer several advantages over synthetic herbicides for weed control, including reduced environmental

* Corresponding author.
E-mail address: fabrizio.araniti@unimi.it (F. Araniti).
[1] Equal contribution.

https://doi.org/10.1016/j.stress.2026.101223
Received 29 October 2025; Received in revised form 20 December 2025; Accepted 3 January 2026
Available online 4 January 2026

persistence, a lower risk of contamination, decreased ecotoxicity, and diverse biochemical modes of action that help minimize the development of resistance in weed populations (Palanivel et al., 2021; Arora et al., 2024). Furthermore, allelochemicals are typically biodegradable, providing opportunities to develop sustainable weed management strategies compatible with integrated pest management practices and organic farming (Macías et al., 2022).

Among plant secondary metabolites, terpenoids represent one of the largest and most chemically diverse groups, with numerous documented phytotoxic activities (Graña et al., 2013; Araniti et al., 2013, 2016, 2017a; Araniti et al., 2017b). Their modes of action involve alterations in critical physiological and metabolic processes, which manifest as disruptions in photosynthetic efficiency, impairment of cellular membrane integrity, induction of oxidative stress, hormonal imbalances, and interference with nutrient uptake and assimilation (Verdeguer et al., 2020).

Nootkatone – a sesquiterpenoid primarily isolated from the peel of grapefruit (*Citrus paradisi*) and Alaskan yellow cedar (*Cupressus nootkatensis*) – has recently attracted scientific interest due to its insecticidal, antimicrobial, aromatic, and food flavoring properties (Panella et al., 2005; Dietrich et al., 2006; Leonhardt and Berger, 2015; Clarkson et al., 2021; Fan et al., 2022; Wang et al., 2022). However, evidence regarding nootkatone's effects on plants remains limited, as few studies have directly investigated its phytotoxic potential, leaving its mode of action and biochemical targets poorly characterized (Mao et al., 2004, 2006; M'Barek, 2016; Habash et al., 2020).

In this study, we present a detailed characterization of the phytotoxic effects exerted by exogenous nootkatone on *Arabidopsis thaliana*. By integrating multiple analytical approaches – including GC–MS-based metabolomics combined with advanced network analysis, stable isotope tracing, and comprehensive nutritional profiling – we formulate a mechanistic hypothesis to explain the toxicity of nootkatone. Specifically, we show that the phytotoxicity of nootkatone is closely linked to its ability to perturb nitrogen nutrition by promoting ammonium uptake over nitrate assimilation, thereby triggering metabolic reprogramming and metabolic stress responses.

Materials and methods

Plant material, growth conditions, and experimental designs

All experiments were carried out on *Arabidopsis thaliana* Col-0 plants that were pre-grown for 25 days in complete nutrient solutions [0.75 mM KNO_3, 0.5 mM $Ca(NO_3)_2$, 1.75 mM NH_4Cl, 1 mM KH_2PO_4, 0.5 mM $MgSO_4$, 0.75 mM KCl, 0.5 mM $CaCl_2$, 25 μM FeNa-EDTA, 46 μM H_3BO_3, 9 μM $MnCl_2$, 0.8 μM $ZnCl_2$, 0.3 μM $CuCl_2$, 0.1 μM $(NH_4)_6Mo_7O_{24}$, 30 μM Na_2SiO_3, pH 6.5], essentially as described by Ferri et al. (2017). The duration of the pre-growing period was selected to ensure the development of well-established hydroponically grown plants, providing sufficient biomass for reliable and reproducible elemental, isotopic, metabolomic, and physiological analyses. At the end of the pre-growing period, plants were transferred to centrifuge tubes containing 50 mL of fresh nutrient solution and incubated for 192 h in the presence or absence of nootkatone at five concentrations (11.25, 22.5, 45, 90, and 180 μM). These concentrations were selected based on: (i) preliminary in vitro dose-response assays on Arabidopsis seedlings grown on agar media, which yielded an estimated IC_{50} of $IC_{50} = 45.7 \pm 4.8$ μM (see, Supplementary Material, Figure S1), and (ii) the estimated aqueous solubility limit of nootkatone, reported to be approximately 36 mg L^{-1} (Zhang et al., 2022). The chosen range therefore encompasses values below and above the experimentally determined EC_{50} while ensuring that concentrations remained below the solubility limit of nootkatone in aqueous solution, thereby avoiding the need for co-solvents.

All hydroponic solutions were renewed daily to minimize nutrient depletion and possible isotopic effects caused by the preferential uptake of lighter ^{14}N isotope (Kalcsits et al., 2014). The renewal procedure did not impose mechanical or cumulative stress, as plants remained undisturbed in their original supports and were handled identically in control and treated groups.

At the end of the exposure period, shoots were harvested, immediately frozen in liquid N_2, ground to a fine powder using a mortar and pestle, and stored at −80 °C until further analysis.

In the ^{15}N-labeled nitrogen experiments, pre-grown plants (as previously described) were either exposed or not exposed to 90 μM nootkatone for 96 h in the same nutrient solution enriched with ^{15}N-NO_3^- at 10 % atomic percentage. Plants were sampled at 24-hour intervals during the incubation. At each time point, roots were washed twice for 10 minutes in ice-cold water to remove apoplastic NO_3^-. Both roots and shoots were then frozen in liquid N_2, ground to a fine powder, and freeze-dried for subsequent analysis of total N content (N_{tot}) and ^{15}N atomic percentage, as described in the section Stable Isotope Analysis. The results were used to calculate the amount of nitrate absorbed during each time interval (Fig. 5D). In the same experiment, the amount of ammonium absorbed during each time interval (Fig. 5E) was estimated as the difference between the change in N_{tot} and the amount of NO_3^- taken up by the plants during each time interval, given that the growth solution contained only NO_3^- and NH_4^+ as absorbable N sources.

Measurement of the chlorophyll fluorescence parameter F_v/F_m

The maximum photochemical quantum yield of photosystem II (F_v/F_m) was measured in treated and untreated *Arabidopsis thaliana* rosettes using an open FluorCam 800 imaging system (Photon System Instruments, Drásov, Czech Republic). Prior to measurement, plants were dark-adapted for 20 min to ensure complete relaxation of the photosynthetic apparatus.

During imaging, cool white LED panels (6500 K; 130 × 130 mm) were positioned at a 45° angle relative to the rosette plane to provide uniform actinic illumination. The camera lens was placed 10–15 cm above the plants to capture the entire rosette surface. The "quenching act 2″ protocol was applied, with a shutter speed of 20 μs and a sensitivity setting of 20 %.

Actinic light was delivered at an intensity of 240 μmol m^{-2} s^{-1}, while saturating pulses were set to 300 μmol m^{-2} s^{-1}. These conditions enabled accurate and reproducible determination of the F_v/F_m parameter.

GC–MS-driven metabolomic analysis

Frozen and pulverized shoot tissue samples were extracted and derivatized following the protocol described by Misra et al. (2020). The derivatized extracts were analyzed using an Agilent 8890 gas chromatograph (Agilent Technologies, USA) coupled to a 5977C single-quadrupole GC/MSD. Sample injections were performed using a CTC PAL autosampler (CTC Analytics, Switzerland). The GC system was equipped with a 30 *m* × 0.25 mm × 0.25 μm 5MS capillary column and a 10 m precolumn. Temperature programs, instrument settings, and MS-DIAL workflows – including baseline correction, alignment, deconvolution, peak detection, and annotation – were applied as described by Misra et al. (2020). Feature annotation was conducted using an in-house spectral library developed according to Misra et al. (2019). To ensure data quality and monitor retention index (RI) drift, solvent blanks, pooled quality control samples, and even-chain C10–C40 n-alkane standards were injected at regular intervals. Metabolite identification was based on matching RI values and electron ionization mass spectra against the proprietary library, with annotations classified as level 2 or 3 according to the criteria established by Sumner et al. (2007). Because GC–MS metabolomics often produces multiple trimethylsilyl (TMS) derivatives of the same metabolite, only the most intense and reproducible derivative was retained for quantitative and multivariate analyses, in accordance with established guidelines. This approach prevents redundant features and ensures data robustness.

Nutrient analysis

For ionome determination, 2 mg of dried and finely ground shoot tissue were digested in 1 mL of a 2:1 (v/v) mixture of nitric acid and perchloric acid. The resulting digests were solubilized in 5 mL of 2 % (v/v) nitric acid and subsequently analyzed by ICP-MS, as described by Orasen et al. (2019). Ammonium content was determined from 150 mg of frozen and pulverized shoot tissue, following the protocol outlined by Prinsi and Espen (2018). Nitrate content was determined from 150 mg of frozen and pulverized shoot tissue according to Cataldo et al. (1975).

Stable isotope analysis

Samples were prepared by placing 1.5 mg of dried and finely ground shoot tissues into 5 × 9 mm tin capsules. Each capsule was sealed using clean tweezers and subsequently loaded into the autosampler. The total nitrogen content and stable nitrogen isotope ratio were determined using a Flash 2000 HT elemental analyzer, coupled via a ConFlo IV interface to a Delta V Advantage Isotope Ratio Mass Spectrometer (IRMS), and controlled through Isodat 3.0 software (Thermo Fisher Scientific). The combustion and reduction reactors, housed within a single quartz tube, were maintained at 1020 °C. Helium was supplied at flow rates of 120 mL min^{-1} for the carrier line and 100 mL min^{-1} for the reference line. For flash combustion, an oxygen purge was applied for 3 s at a flow rate of 175 mL min^{-1} per sample. The gas chromatographic (GC) separation column was held at 45 °C. At the start of each run, three 20-second pulses of N_2 reference gas were introduced. The total run time for each sample analysis was 600 s. Calibration was carried out using secondary reference materials provided by IAEA: IAEA-N-1 ($\delta^{15}N = +0.43 \pm 0.07$ ‰); IAEA-N-2 ($\delta^{15}N = +20.41 \pm 0.12$ ‰); IAEA-N-3 ($\delta^{15}N = +4.7 \pm 0.2$ ‰). Two in-house standards – sulfanilamide ($\delta^{15}N = +4.12 \pm 0.1$ ‰) and methionine ($\delta^{15}N = +6.12 \pm 0.1$ ‰) – were used for normalization and quality assurance. Isotope ratios were expressed in delta (δ) notation in parts per thousand (‰), relative to the international standard – the atmospheric nitrogen (AIR) – as follows:

$$\delta^{15}N_{AIR}(‰) = \left(R_{sample} - R_{standard}\right)/\left(R_{standard}\right) \times 1000$$

where R is the ratio of the heavy to light isotope in the sample and the standard.

Statistical analysis

Metabolomic experiments were conducted using a completely randomized design with three biological replicates. Prior to multivariate and univariate statistical analyses, metabolite intensities extracted via MS-DIAL were normalized to the ribitol internal standard, log_{10}-transformed, and Pareto scaled. All data preprocessing was performed using the open-source platform MetaboAnalyst 6.0 (Pang et al., 2024). Following normalization, unsupervised principal component analysis (PCA) and supervised partial least squares discriminant analysis (PLS-DA) were performed to identify and visualize metabolic shifts among experimental groups. In the PLS-DA model, the variable importance in projection (VIP) score was used to quantify the contribution of each metabolite to group separation; metabolites with VIP scores > 1 were considered significant contributors. Permutational multivariate analysis of variance (PERMANOVA) was applied to the principal component scores to assess differences among predefined groups, using 999 random permutations. To prevent overfitting, the PLS-DA model was validated through cross-validation and permutation testing (20 permutations). The model was considered valid only when empirical *P*-values for both Q^2 and R^2Y were ≤ 0.05 and their values approached 1.

Subsequently, pairwise partial correlations between metabolites were calculated using debiased sparse partial correlation (DSPC), applying a betweenness centrality threshold of 1 to evaluate relationships between individual metabolites while accounting for the influence of all others (Basu et al., 2017). Univariate analysis was performed using one-way ANOVA followed by Fisher's least significant difference (LSD) post hoc test, with statistical significance set at $P \leq 0.05$. Quantitative data for all other measurements are presented as mean ± standard deviation (SD). Significance values were adjusted for multiple comparisons using the Bonferroni correction. Student's *t*-test was used to assess differences between control and nootkatone-treated plants, with statistical significance defined as $P < 0.05$.

Results

Nootkatone exposure reduces biomass and impairs photosynthetic efficiency in Arabidopsis

Arabidopsis plants exposed to increasing concentrations of nootkatone (0–180 μM) for 192 h exhibited a concentration-dependent reduction in both root and shoot biomass accumulation (Fig. 1A,B). Photosynthetic performance – evaluated through the maximum photochemical quantum yield of photosystem II (F_v/F_m) – also declined in a dose-dependent manner (Fig. 1C). Significant reductions in F_v/F_m values were observed at concentrations ≥ 45 μM, indicating impaired photosynthetic efficiency in response to nootkatone exposure. The visual assessment of rosette morphology at the end of the treatment period aligned with the physiological data (Fig. 1D). Control plants (0 μM) and those treated with 11.25 μM nootkatone exhibited healthy and fully expanded green rosettes. In contrast, plants exposed to nootkatone concentrations ≥ 45 μM showed progressive reductions in size, chlorosis, and necrosis, particularly at 90 and 180 μM, consistent with stress-induced damage.

Nootkatone induces dose-dependent metabolic reprogramming centered on amino acid metabolism

Principal component analysis (PCA) of the metabolite profiles revealed a clear dose-dependent separation of Arabidopsis metabolomes along the first two components (Fig. 2A). PERMANOVA performed on the PCA results yielded an F-value of 8.0288, an R^2 of 0.76987, and a *P*-value of 0.001 (based on 999 permutations), indicating strong separation among predefined groups in multivariate space (high F), with approximately 67 % of the total variance explained (high R^2), and a highly significant grouping pattern unlikely to have occurred by chance ($P = 0.001$). The three biological replicates for each nootkatone treatment clustered tightly, indicating high experimental and analytical repeatability. Principal component 1 (PC1) accounted for 48.7 % of the total variance and primarily separated the highest nootkatone concentrations (90 and 180 μM) from both the control (0 μM) and low-dose treatments (11.25 and 22.5 μM). Principal component 2 (PC2) explained an additional 18.6 % of the variance, further distinguishing the intermediate concentration (45 μM) from the extremes (Fig. 2A). Collectively, the first two principal components accounted for the majority of metabolic alterations induced by nootkatone exposure, highlighting a concentration-dependent reprogramming of the Arabidopsis metabolome (Fig. 2A). The PC1 loading vector was primarily defined by metabolites such as citrulline, glutamine, L-ornithine, tryptophan, citric acid, asparagine, and pantothenic acid. In contrast, PC2 was mainly driven by fumaric acid, mannitol, galactose, fructose, methylsuccinic acid, threonic acid, L-ornithine, β-alanine, urea, phosphate, and sorbitol (Fig. 2B; Table S1).

Since PCA provided an unbiased overview of variance and confirmed dose-dependent metabolic trends without incorporating class information, supervised PLS-DA was subsequently applied to maximize group separation, identify key discriminant metabolites through variable importance in projection (VIP) scores, and enhance the interpretability of dose-related metabolic signatures. The supervised PLS-DA model, constructed using the same dataset, enhanced and substantiated the dose-dependent clustering initially observed through PCA by leveraging

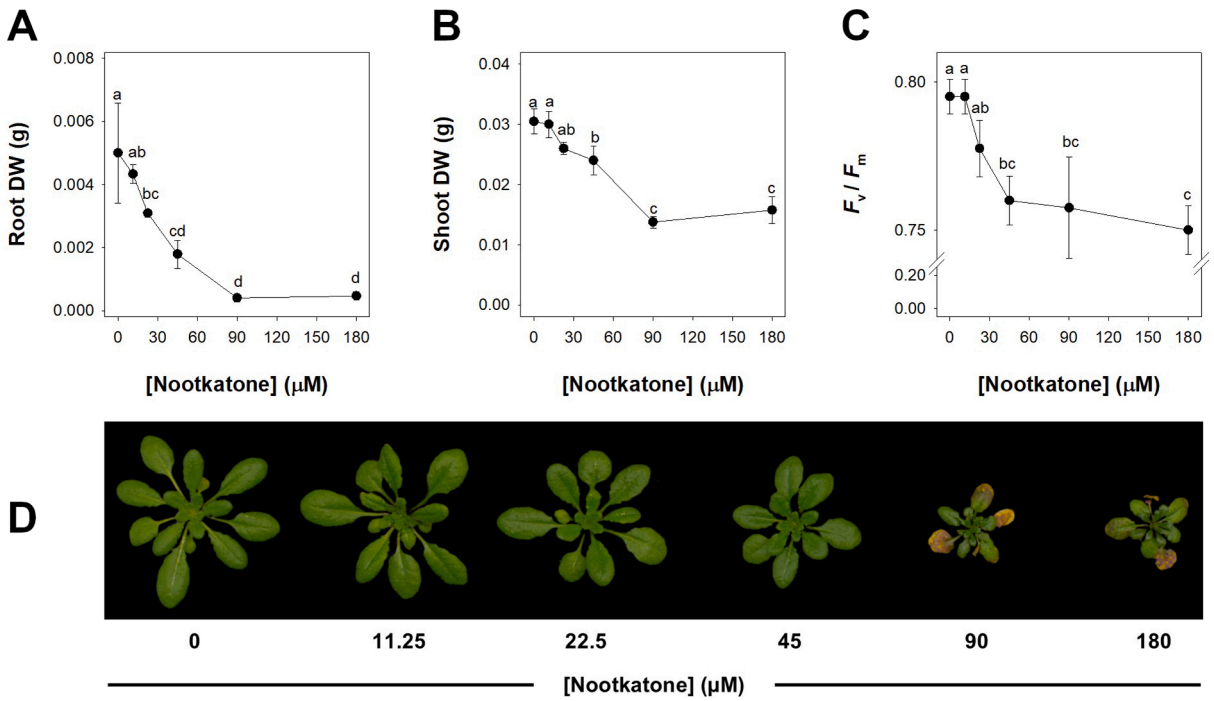

Fig. 1. Growth and chlorophyll fluorescence of Arabidopsis plants exposed to increasing nootkatone concentrations. Plants were exposed to increasing concentrations of nootkatone (0–180 μM) for 192 h. (A) Root dry weight. (B) Shoot dry weight. (C) Dark-adapted maximum photochemical quantum yield of photosystem II (F_v/F_m). (D) Arabidopsis rosettes at the end of nootkatone exposure. Data are the mean and SD of two experiments run in quadruplicate ($n = 8$). Different letters indicate significant differences ($P < 0.05$). DW, dry weight.

known treatment labels to optimize inter-class variance. While PCA began to differentiate between high and low nootkatone concentrations, PLS-DA yielded more compact and clearly separated clusters across all six tested concentrations (0–180 μM). This was evidenced by elevated R^2Y and Q^2 values (approaching 1) and a score plot exhibiting no overlap between groups (Fig. 2C; Table S1). Model robustness was confirmed through cross-validation and a 20-fold permutation test, with empirical *P*-values ≤ 0.05 for both Q^2 and R^2Y, indicating the absence of overfitting (Table S1). Furthermore, the 334 metabolites with VIP scores exceeding 1 were categorized into distinct chemical classes (Fig. 2D). Amino acids and their derivatives, which represented the most abundant class of metabolites, included citrulline, tryptophan, glutamine, L-ornithine, asparagine, glutamic acid, L-aspartic acid, L-serine, proline, γ-aminobutyric acid (GABA), and pyroglutamic acid. Tricarboxylic acid (TCA) cycle intermediates included citric acid and malic acid. Sugars and sugar derivatives comprised glucose, xylulose, and β-lactose. Phenolic and phenylpropanoid compounds consisted of sinapinic acid and 1,4-benzenedicarboxylic acid. Glucosinolates and indolic compounds were represented by sinigrin and 3-indoleacetonitrile. The pyrimidine derivative 5,6-dihydrouracil and the polyamine spermidine were also detected. Lipid-related metabolites included long-chain alkanes (tricosane, heneicosane, tetracosane, and pentacosane) and fatty acids (heptadecanoic, nonadecylic, stearic, and icosanoic acids). Pantothenic acid was the only compound identified in the cofactor-related category.

The heatmap adjacent to the VIP score plot illustrates the concentration changes of each metabolite across the entire range of nootkatone contractions tested (Fig. 2D). Notably, most of the amino acids were characterized by a dose-dependent increase. In addition, ANOVA revealed that 51 out of 81 metabolites were significantly affected by the treatments. These metabolites were visualized in a heatmap (Fig. 3), which displays their relative scaled abundances (rows) across the six nootkatone treatment groups. Hierarchical clustering was applied to both metabolites and samples. In the sample dendrogram (top), the highest concentrations (90 and 180 μM) formed a distinct cluster, clearly separated from the control group and the lower to intermediate concentrations (classes 11.25 and 22.50 μM) (Fig. 3). Metabolites were grouped into three major clusters, as shown in the left dendrogram. The uppermost cluster predominantly comprised metabolites that were upregulated (red) at the highest nootkatone concentrations and downregulated (blue) at lower doses. In contrast, the lowermost cluster exhibited the opposite trend, with the highest relative abundances observed in control and low-dose treatments, and reduced levels at higher concentrations. The intermediate cluster displayed more subtle shifts, characterized by moderate changes in abundance across the mid-range treatments.

The debiased sparse partial correlation (DSPC) network was found to be organized around a central cluster of amino acids and related metabolites. 1,4-Benzenedicarboxylic acid [degree = 10; betweenness = 27.17] and pantothenic acid [degree = 9; betweenness = 20.26] showed the highest connectivity and centrality, indicating a key role in linking different regions of the network (Fig. 4, Table S2). However, several amino acids were identified as major hubs. Asparagine [degree = 8; betweenness = 48.4], L-aspartic acid [degree = 8; betweenness = 26.14], glutamine [degree = 9; betweenness = 19.58], and glutamic acid [degree = 6; betweenness = 21.71] were located in the dense core of the network, where strong positive associations were concentrated. Their position reflects the central involvement of amino acid metabolism in maintaining network connectivity. High betweenness values were also recorded for citrulline [degree = 4; betweenness = 18] and GABA [Degree = 3; Betweenness = 20], suggesting that these metabolites act as bridges between amino acid metabolism and other biochemical processes (Fig. 4, Table S2). Peripheral structures were observed in contrast to the amino acid-rich core. Hydrocarbons such as heneicosane [degree = 2; betweenness = 0] and tricosane [degree = 2; betweenness = 0] formed an isolated cluster, showing limited integration with the main network. In addition, organic acids such as malic acid [degree = 7; betweenness = 42.14] and glycolic acid [degree = 8; betweenness = 38.4] displayed the highest betweenness overall, indicating a bridging role between the amino acid cluster and pathways

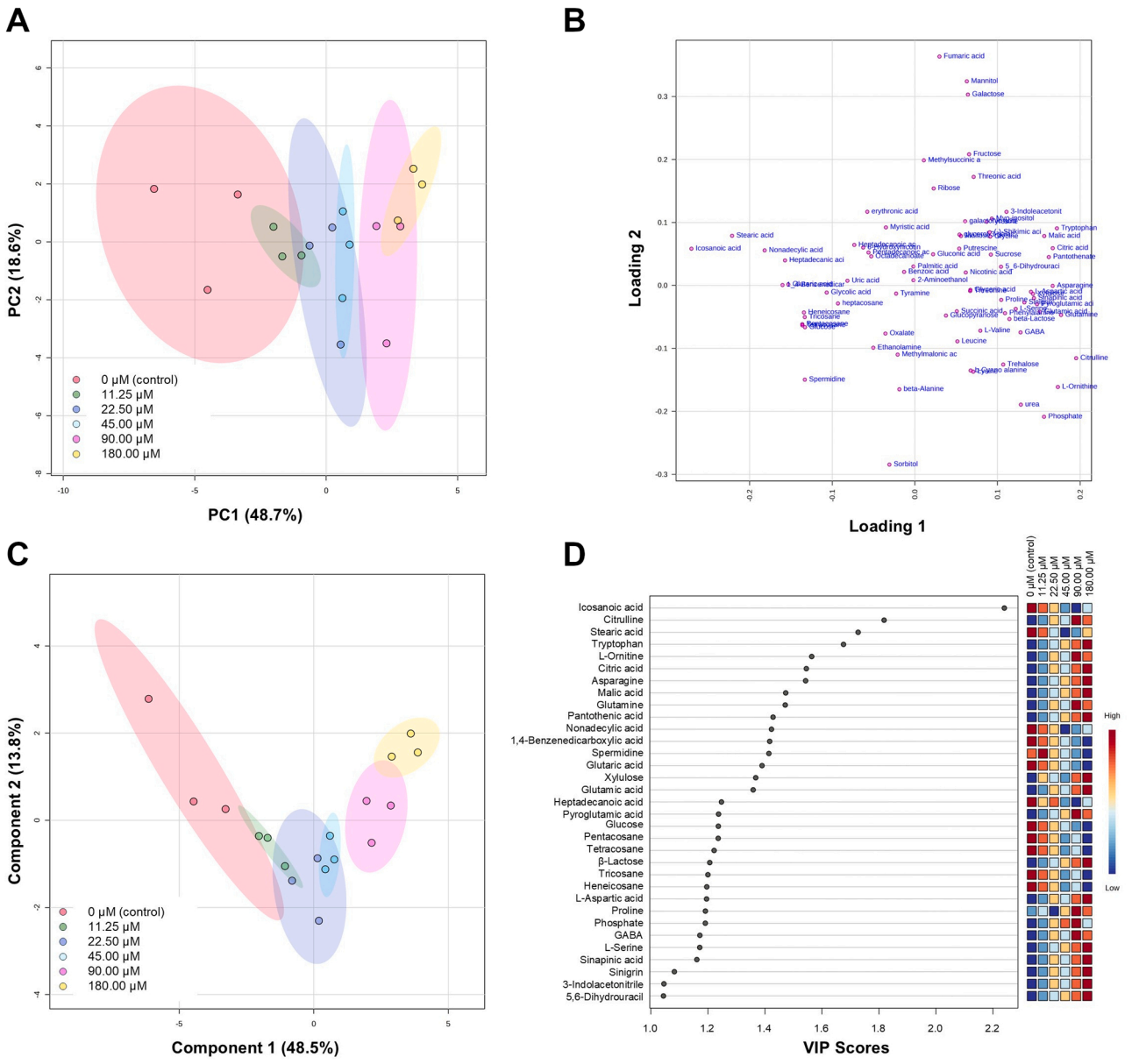

Fig. 2. Multivariate analysis of metabolomic responses in shoots of Arabidopsis plants exposed to increasing nootkatone concentrations. Plants were exposed to 0 µM (red), 11.25 µM (green), 22.5 µM (blue), 45 µM (cyan), 90 µM (magenta) and 180 µM (yellow) nootkatone for 192 h. Metabolite profiling was performed by gas chromatography–mass spectrometry (GC–MS). Each treatment group included three biological replicates ($n = 3$). (A) Principal component analysis (PCA) score plot showing unsupervised clustering of samples. Principal components 1 and 2 explain 49.0 % and 18.5 % of the total variance, respectively. (B) Corresponding PCA loading plot indicating the contribution of individual metabolites to the separation of samples. (C) Partial least-squares discriminant analysis (PLS-DA) score plot showing supervised separation of the six treatment groups. Component 1 and component 2 explain 48.9 % and 13.8 % of the variance, respectively. Ellipses represent 95 % confidence intervals for each group. (D) Variable Importance in Projection (VIP) scores for metabolites with VIP > 1, ranked from highest to lowest. Each dot represents one metabolite. The adjacent heatmap displays normalized abundances of these VIP-selected metabolites across the six treatment groups, highlighting dose-dependent changes in metabolite levels. The raw data and statistics are reported in Table S1.

linked to carbohydrate and energy metabolism (Fig. 4, S2).

Nootkatone disrupts nitrogen uptake and mineral nutrient homeostasis

The impact of increasing concentrations of nootkatone on the nutritional status of Arabidopsis plants was assessed by quantifying the accumulation of various mineral nutrients in rosette tissues. For these experiments, plants were grown in a complete hydroponic solution containing three distinct sources of inorganic nitrogen, each characterized by a specific natural-abundance isotopic signature: 0.5 mM $Ca(NO_3)_2$ ($\delta^{15}N = 2.63 \pm 0.06$ ‰), 0.75 mM KNO_3 ($\delta^{15}N = 3.78 \pm 0.11$ ‰), and 1.75 mM NH_4Cl ($\delta^{15}N = -10.23 \pm 0.25$ ‰). The $\delta^{15}N$ value of the total nitrogen pool in the nutrient solution was -3.55 ± 0.06 ‰. The use of nitrogen sources with distinct isotopic signatures at natural abundance enabled the estimation of the relative contribution of each nitrogen form (nitrate and ammonium) to the total nitrogen accumulated in rosette tissues.

Increasing concentrations of nootkatone did not significantly affect total nitrogen levels, except at the highest dose tested, which resulted in a 39 % reduction compared to the untreated control (Fig. 5A). Shoot nitrate levels decreased significantly in a dose-dependent manner with increasing nootkatone concentrations (Fig. 5B). By contrast, a significant increase in shoot ammonium levels was observed following nootkatone exposure; for example, at 45 µM, ammonium concentration was

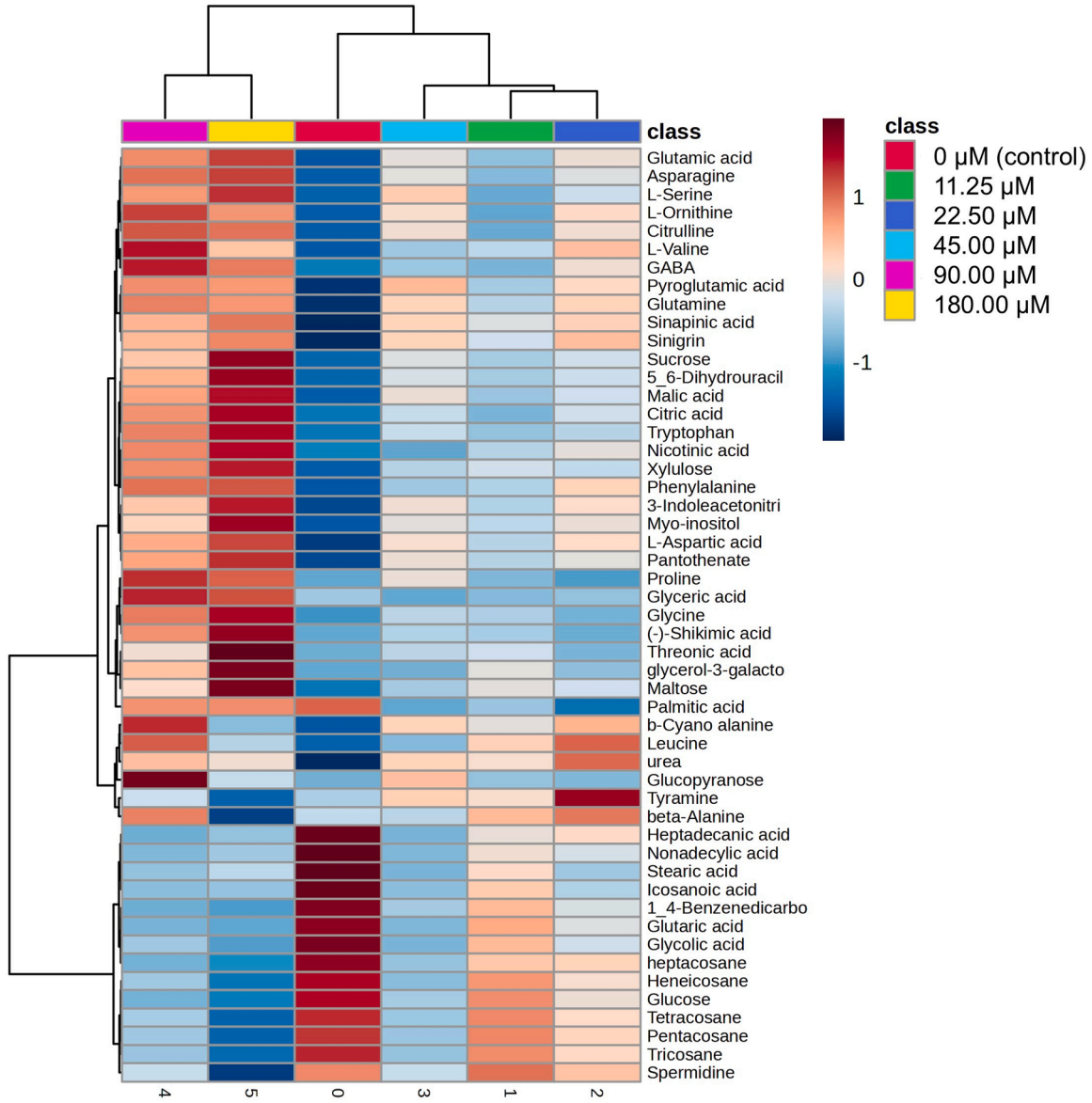

Fig. 3. Heatmap of metabolites significantly affected by nootkatone exposure in Arabidopsis. Metabolites showing significant differences among treatments were identified by one-way ANOVA followed by Fisher's LSD post-hoc test ($P \leq 0.05$). The heatmap displays normalized intensities of 52 metabolites (rows) that differed significantly in shoots of Arabidopsis plants exposed to increasing concentrations of nootkatone (from 0 to 180 µM) for 192 h (columns). Each class includes three biological replicates ($n = 3$). Hierarchical clustering of both metabolites and treatment groups was performed using Euclidean distance and Ward's linkage method. The colour gradient (blue to red) represents relative metabolite abundance within each treatment group, with red indicating higher and blue indicating lower levels. The raw data and statistics are reported in Table S1.

2.4-fold higher than in control plants (Fig. 5C).

Isotopic analyses revealed that shoot tissues were consistently depleted in ^{15}N relative to the nutrient solution. The $\delta^{15}N$ values progressively decreased with increasing nootkatone concentrations, ultimately approaching the isotopic signature of the ammonium source in the medium (Fig. 5D).

Significant effects of nootkatone exposure were also observed on the homeostasis of several mineral nutrients in shoot tissues (Fig. 6), including phosphorus (P), potassium (K), calcium (Ca), magnesium (Mg), iron (Fe), and molybdenum (Mo). The concentrations of specific elements exhibited dose-dependent trends, with Fe levels increasing and K, Ca, Mg, and Mo levels decreasing as nootkatone concentrations in the growth medium increased.

Nootkatone alters nitrogen source preference by promoting ammonium over nitrate uptake

Based on nitrogen-related data suggesting that nootkatone may alter the relative uptake of nitrate and ammonium, a ^{15}N-labeled nitrogen experiment was set up to further investigate its influence on the assimilation of these two inorganic nitrogen sources. In this experiment, Arabidopsis plants previously grown under standard hydroponic conditions were incubated for 96 h in a nutrient solution enriched with ^{15}N-NO_3^- (10 atom %), either in the absence or presence of 90 µM nootkatone. The results indicated that nootkatone did not significantly affect total nitrogen accumulation in whole plants throughout the incubation period (Fig. 7A). A similar trend was observed when roots and shoots were analyzed separately, suggesting that nootkatone did not alter total nitrogen partitioning within the plant (Fig. 7B,C). However, its presence in the growth medium significantly influenced the relative utilization of

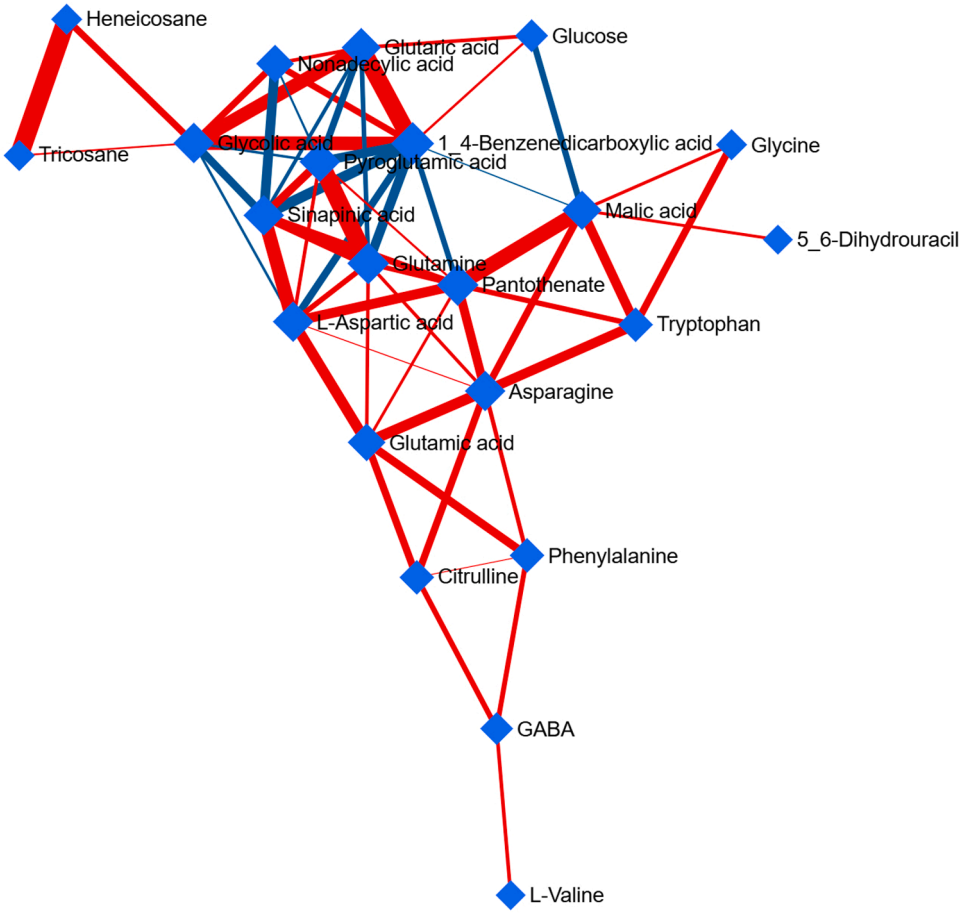

Fig. 4. Correlation network of metabolites distinguishing nootkatone-treated from untreated Arabidopsis plants. The network was generated using the DSPC algorithm based on metabolites that significantly differentiated nootkatone-treated plants from controls ($n = 3$). Blue nodes represent individual metabolites. Red edges indicate positive correlations, while blue edges indicate negative correlations between metabolite pairs. The raw data and statistics are reported in Table S1.

the two inorganic nitrogen sources, repressing nitrate absorption while promoting ammonium uptake (Fig. 7D,E). These responses were associated with changes in ammonium accumulation in shoot tissues, which were significantly higher in plants exposed to nootkatone (Fig. 7F).

Discussion

Exposure of *Arabidopsis thaliana* to increasing concentrations of nootkatone produced marked phytotoxic effects, as evidenced by a dose-dependent reduction in plant biomass and visible morphological damage to rosette tissues (Fig. 1). The first visible symptoms appeared at 45 μM – a relatively low concentration compared to those typically required to elicit significant effects from other plant specialized metabolites (Graña et al., 2013; Araniti et al., 2017b; López-González et al., 2020) – and progressively intensified at 90 and 180 μM, culminating in severe leaf chlorosis and necrosis (Fig. 1D). Comparable outcomes have been widely reported in Arabidopsis plants treated with other terpenoids (Graña et al., 2013; Araniti et al., 2017b, 2020; Landi et al., 2020). Such a behavior likely reflects a state of acute stress, as further evidenced by a marked decline in the chlorophyll fluorescence parameter F_v/F_m at nootkatone concentrations $\geq$ 45 μM (Fig. 1C). This reduction indicates a substantial impairment of the photosynthetic apparatus, particularly photosystem II (PSII), consistent with responses previously reported for other natural phytotoxic compounds, driven by the accumulation of reactive oxygen species (ROS) and the resulting damage to the antenna complex (Hejl et al., 1993; Hussain et al., 2011; Uddin et al., 2012; Araniti et al., 2018; Dalal et al., 2018; Hussain and Reigosa, 2021).

To elucidate the metabolic pathways involved in nootkatone-induced phytotoxicity, a comprehensive metabolomic analysis was performed using gas chromatography–mass spectrometry (GC–MS). The results revealed clear dose-dependent metabolic alterations, indicating significant disruptions in primary metabolic processes (Fig. 2; Fig. 3). Integration of metabolomic data with DSPC network analysis enabled the identification of critical metabolic nodes and the mapping of connections among key metabolites, thereby revealing perturbations at the biochemical pathway level (Fig. 4). This statistical approach enabled the reconstruction of sparse networks by estimating direct associations between metabolites, thereby reducing spurious correlations and providing a more reliable view of their functional interconnections (Basu et al., 2017). Network analysis identified glutamic acid as a metabolite with high connectivity and centrality, suggesting its role as a key metabolic hub. In this context, the degree – a measure of the number of direct connections a node possesses – highlights hub metabolites that coordinate multiple pathways. Meanwhile, betweenness centrality quantifies the role of a metabolite in bridging distinct clusters, identifying compounds that act as biochemical mediators between different metabolic routes. These parameters are particularly valuable for spotting key metabolites that orchestrate pathway reprogramming under stress conditions (Basu et al., 2017). In plants, glutamic acid plays a central role in nitrogen metabolism, functioning as a precursor or intermediate in the biosynthesis of amino acids, nitrogen-containing secondary metabolites, and signaling molecules (Forde and Lea, 2007).

The identification of significant correlations between amino acids and phenolic metabolites, such as sinapic acid, underscores the potential interaction between primary nitrogen metabolism and secondary metabolic pathways, possibly reflecting the plant's attempt to cope with

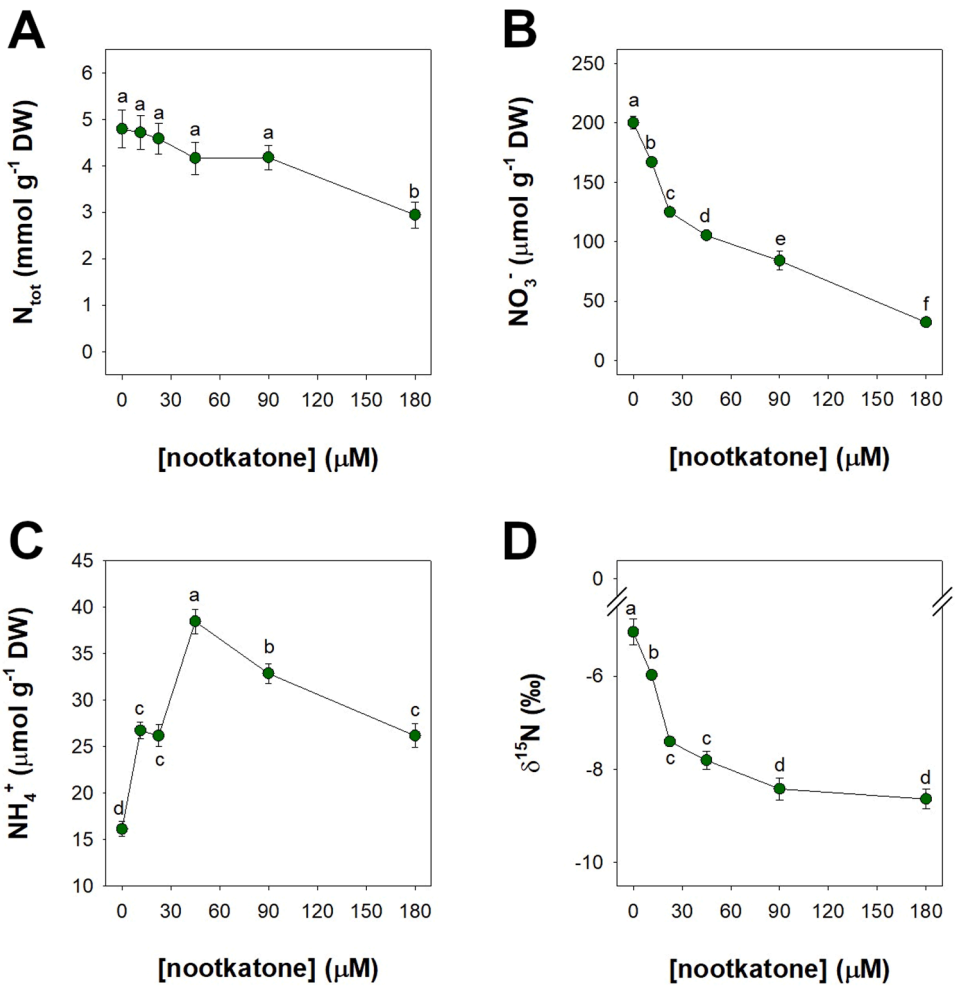

Fig. 5. Nitrogen nutritional status and stable nitrogen isotope composition in shoots of Arabidopsis exposed to increasing nootkatone concentrations. Plants were exposed to increasing concentrations of nootkatone (0–180 μM) for 192 h. (A) Total nitrogen concentration. (B) Nitrate concentration. (C) Ammonium concentration. (D) Stable nitrogen isotope composition ($\delta^{15}N$). Data are the mean and SD of two experiments run in quadruplicate ($n = 8$). Different letters indicate significant differences ($P < 0.05$). DW, dry weight.

the stress condition through activation of protective metabolic routes (Widhalm and Dudareva, 2015). Moreover, the presence of peripheral metabolite clusters, including lipophilic compounds such as tricosane and heneicosane, suggests broader metabolic reprogramming potentially involving alterations in cell membrane integrity and activation of oxidative stress responses, processes commonly affected under toxic conditions (Chaimovitsh et al., 2017; Araniti et al., 2018; Verdeguer et al., 2020). In this context, the observed increase in GABA – a known stress-responsive metabolite – may further support the hypothesis of a generalized effect of nootkatone on the plant's redox status (Rastegar and Sayyad-Amin, 2025). Collectively, the DSPC network analysis highlights a multifaceted impact of nootkatone, with a predominant focus on nitrogen-related metabolic processes. Similar alterations in nitrogen metabolism have been reported following exposure to other natural allelochemicals, including coumarin (Chen et al., 2011; Zhou et al., 2013; Lupini et al., 2018), dihydrodiconiferyl alcohol and lariciresinol (Carillo et al., 2010), and p-hydroxybenzoic acid (Yu et al., 2020).

Besides its notable effects on the levels of certain nitrogen-containing organic compounds, such as amino acids, nootkatone exposure significantly impacted nitrogen nutrition and ionic homeostasis in Arabidopsis plants (Fig. 5; Fig. 6). One of the most striking responses was a substantial shift in the nitrate-to-ammonium ratio in shoot tissues. Under control conditions (i.e., in the absence of nootkatone), this ratio was approximately 12.4; however, it declined sharply to around 1.2 at the highest nootkatone concentration analyzed. This shift was primarily driven by a sharp decrease in nitrate accumulation, accompanied by a comparatively moderate increase in ammonium accumulation (Fig. 5). Although these two inorganic nitrogen forms are metabolically interconnected – since ammonium can be generated via nitrate reduction (Salsac et al., 1987; Hawkesford et al., 2023) – the observed pattern does not appear to result from enhanced nitrate reduction activity in the plants. This interpretation is further supported by N stable isotope analysis in natural abundance, which revealed a dose-dependent shift in the $\delta^{15}N$ signature of shoot tissues toward the isotopic composition of the ammonium source present in the hydroponic solution (Fig. 5D). These results reinforce the hypothesis that nootkatone modulates the relative uptake of nitrate and ammonium, rather than affecting nitrate reduction processes within plant tissues. In other words, nootkatone appears to influence the plant's capacity to selectively absorb the two inorganic nitrogen sources when both are simultaneously available in the growth medium. This shift in nitrogen source preference was corroborated by ^{15}N-labeled experiments, which enabled direct quantification of a marked reduction in ^{15}N-NO_3^- uptake in the presence of nootkatone (Fig. 7D). Notably, this reduction was not associated with changes in the total nitrogen content of the plant (Fig. 7A), suggesting that the decreased nitrate uptake was compensated by enhanced ammonium absorption (Fig. 7E).

Within this logical framework, increased ammonium uptake may represent a key upstream event in a possible cause-effect relationship,

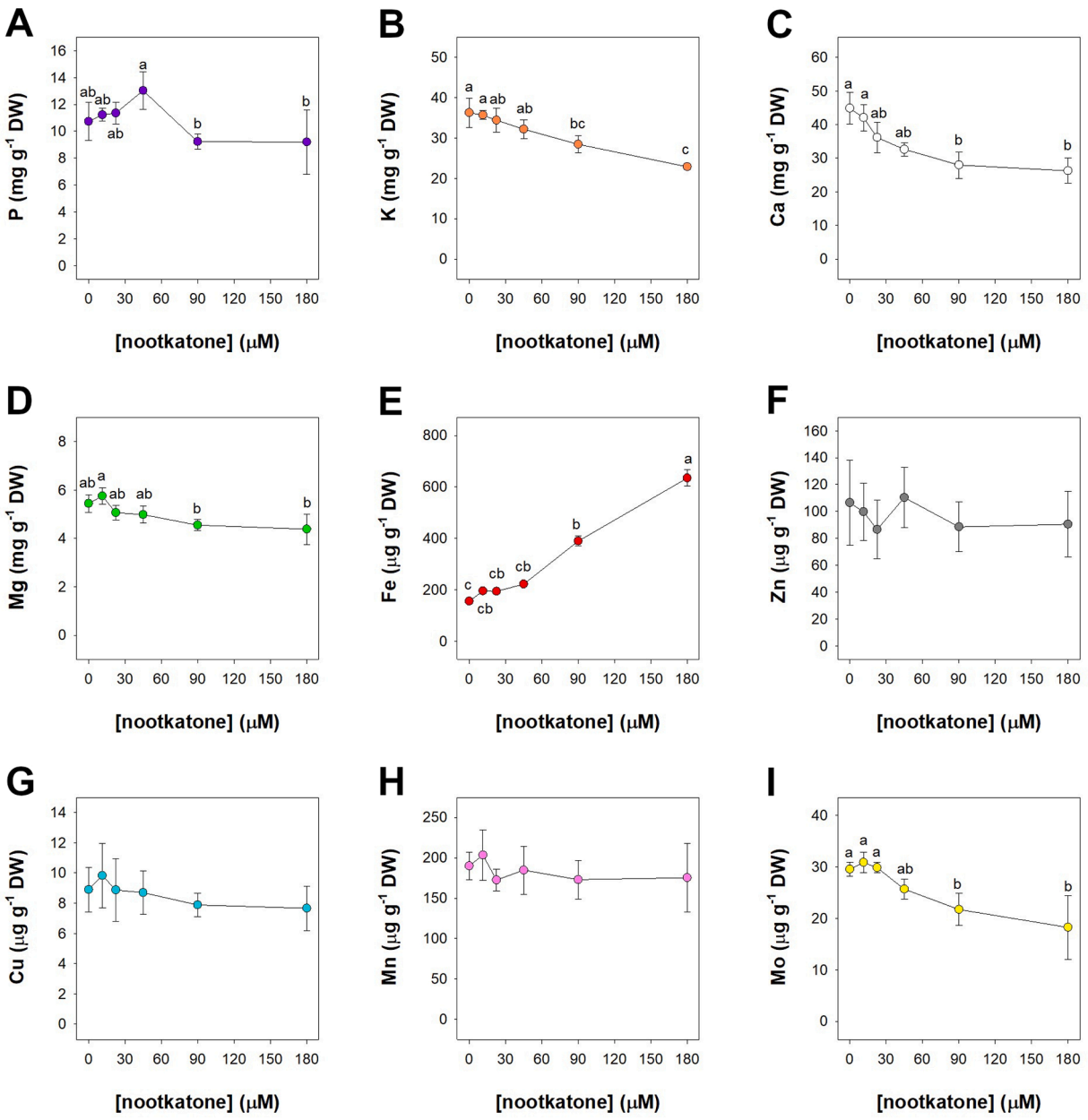

Fig. 6. Elemental composition in shoots of Arabidopsis exposed to increasing nootkatone concentrations. Plants were exposed to increasing concentrations of nootkatone (0–180 μM) for 192 h. (A) Phosphorus. (B) Potassium. (C) Calcium. (D) Magnesium. (E) Iron. (F) Zinc. (G) Copper. (H) Manganese. (I) Molybdenum. Data are the mean and SD of two experiments run in quadruplicate ($n = 8$). Different letters indicate significant differences ($P < 0.05$). DW, dry weight.

whereby elevated ammonium levels stimulate the synthesis of amino acids and other nitrogen-containing metabolites. This interpretation is consistent with the metabolic reprogramming observed in nootkatone-treated plants (Fig. 2; Fig. 3). In other words, these alterations may primarily result from a physiological condition induced by an imbalanced utilization of the two nitrogen forms, a phenomenon commonly referred to as ammonium toxicity (Britto and Kronzucker, 2002; Esteban et al., 2016; Xiao et al., 2023). The manifestation of typical symptoms associated with ammonium toxicity – such as leaf chlorosis, necrosis, and stunted growth – often reflects a complex physiological syndrome, the components of which are partially mirrored in the metabolic and physiological profiles observed in nootkatone-exposed plants.

The accumulation of free amino acids in plant tissues is frequently observed when ammonium is supplied as the sole nitrogen source, in comparison to conditions where nitrate is provided alone (Harada et al., 1968; Magalhaes and Wilcox, 1984; Blacquière et al., 1988; Majerowicz et al., 2000; Domínguez-Valdivia et al., 2008). A fully consistent pattern was observed in the present study, whereby a substantial number of amino acids accumulated in shoot tissues in relation to the external concentration of nootkatone and the accumulation of ammonium in shoot tissues (Fig. 3, Fig. 5C). This accumulation appears to be linked to the rapid assimilation of absorbed ammonium in response to a stress condition or a metabolic imbalance, as it did not lead to enhanced growth, but rather to its inhibition (Fig. 1), an outcome typically associated with ammonium toxicity (Britto and Kronzucker, 2002). Finally, ammonium stress in plants is often associated with the accumulation of nitrogen-rich intermediates such as L-ornithine and citrulline, which serve as key nodes in both nitrogen detoxification and polyamine biosynthesis pathways (Urra et al., 2022; Buezo et al., 2025). However, the observed increase in GABA – a product of polyamine catabolism – suggests that, under nootkatone-induced stress, plants may prioritize the accumulation of putrescine-derived catabolites as part of a rapid stress

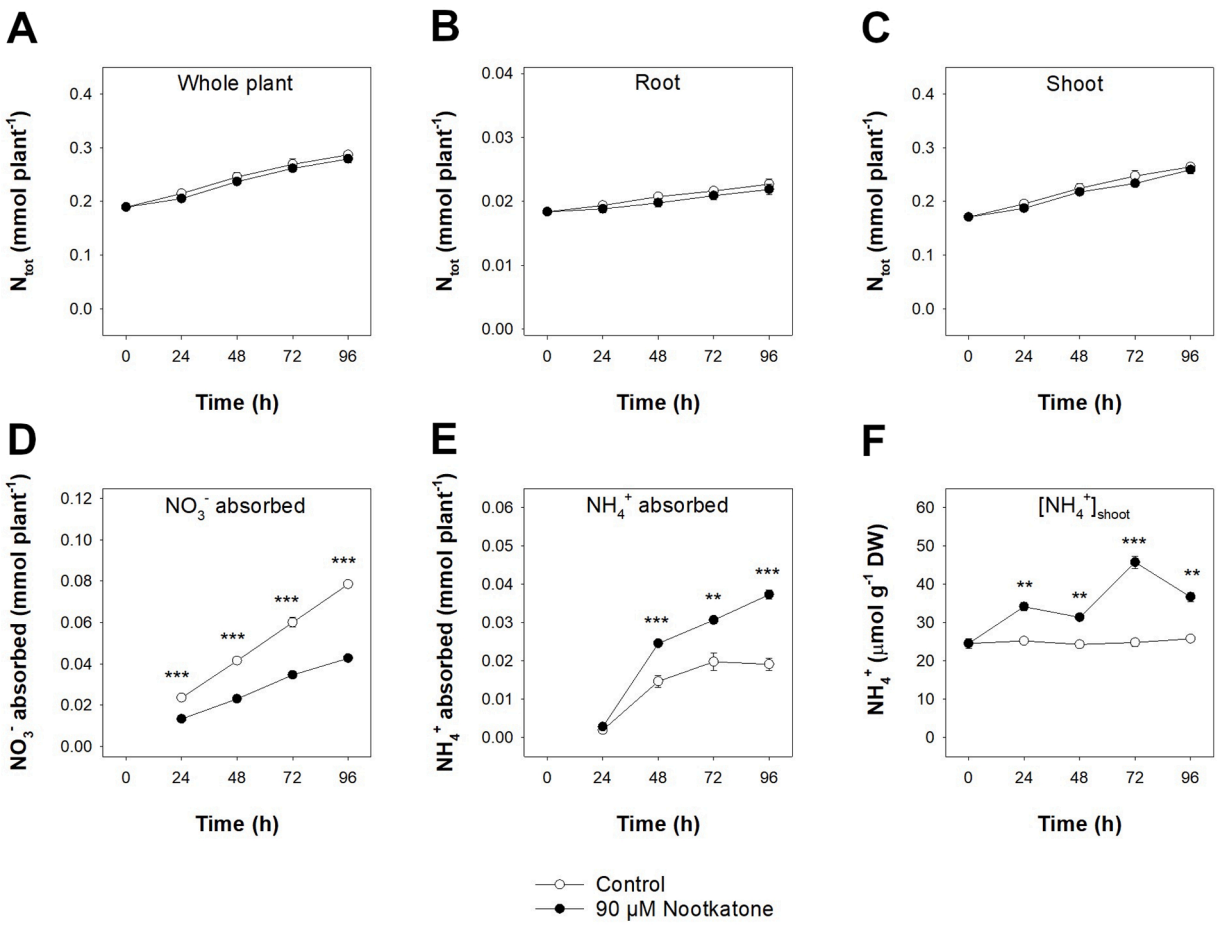

Fig. 7. Time course of nitrogen accumulation and nitrate and ammonium absorption in Arabidopsis plants exposed to nootkatone. Plants were incubated for 96 h in a nutrient solution enriched with ^{15}N-NO_3 (10 atom %), either in the absence or presence of 90 µM nootkatone. (A) Total nitrogen in the whole plant. (B) Total nitrogen in root tissues. (C) Total nitrogen in shoot tissues. (D) NO_3 absorbed from the growth medium. (E) NH_4^+ absorbed from the growth medium. (F) NH_4^+ accumulation in the shoot tissues. Data are the mean and SD of two experiments run in quadruplicate ($n = 8$). Different letters indicate significant differences ($P < 0.05$). Asterisks indicate significant differences between PF and AWD (Student's *t*-test; * $P \leq 0.05$, ** $P \leq 0.01$, *** $P \leq 0.001$). DW, dry weight.

response. The concurrent reduction in spermidine levels, despite elevated concentrations of upstream precursors such as L-ornithine and citrulline, may reflect a strategic metabolic shift favoring immediate stress mitigation over long-term growth-related functions (Fig. 3).

The high ammonium concentration is consistent with the observed decrease in the levels of key cations – such as potassium (K^+), calcium (Ca^{2+}), and magnesium (Mg^{2+}) – in the shoot tissues of nootkatone-treated plants (Fig. 6). This pattern is a well-documented symptom of ammonium stress in plants, wherein excessive ammonium uptake disrupts ionic balance and interferes with the acquisition of essential cations (Van Beusichem et al., 1988; Coskun et al., 2013; Coleto et al., 2023; Wdowiak et al., 2024). In this study, a dose-dependent increase in iron concentration was observed in the shoot tissues of Arabidopsis plants exposed to increasing levels of nootkatone (Fig. 6E). This finding is consistent with the mechanistic framework recently described in Arabidopsis, whereby ammonium-based nutrition disrupts iron homeostasis, leading to excessive iron accumulation, particularly under conditions of impaired nitrate uptake, as observed in the present work (Li et al., 2025). Finally, the reduced accumulation of molybdenum in shoot tissues may be indirectly associated with the negative effect of nootkatone on nitrate uptake (Fig. 6I). The resulting decrease in cellular nitrate availability could, in turn, lower the demand for the molybdenum cofactor (Moco), which is essential for nitrate reductase activity (Hewitt and Gundry, 1970; Mendel and Hänsch, 2002).

Under ammonium stress, the reduction in inorganic cation levels is often accompanied by a depletion of TCA cycle intermediates and disturbances in pH regulation processes (Britto and Kronzucker, 2005; Hachiya et al., 2021; Xiao et al., 2023). However, our results indicate that following exposure to increasing concentrations of nootkatone, the ammonium toxicity profile is associated with a progressive increase in the levels of certain TCA cycle intermediates, such as citric acid and malic acid (Fig. 3). This apparent inconsistency is likely due to the fact that the nootkatone treatments were conducted in hydroponic solutions containing equal concentrations of nitrate and ammonium (1.75 mM each). It is indeed well known that under co-provision conditions, small amounts of nitrate can mitigate ammonium toxicity in several species, including Arabidopsis (Xiao et al., 2023). It has been shown that nitrate supply can accelerate ammonium assimilation and promote the synthesis of organic acids in the TCA cycle, which are essential to sustain amino acid biosynthesis (Du et al., 2021). This effect is likely due to the fact that nitrate reduction, being a proton-consuming activity, mitigates the acidic stress caused by ammonium assimilation (Britto and Kronzucker, 2005; Hachiya et al., 2021). This mechanism helps maintain pH homeostasis and creates conditions favorable for organic acid synthesis, likely through the activation of pH-stat mechanisms such as those involving phosphoenolpyruvate carboxylase (Davies, 1986; Britto and Kronzucker, 2005). Within this conceptual framework, the different proton balance achievable under co-provision conditions could explain the effect of nootkatone on the accumulation of organic acids in Arabidopsis shoots. Although the majority of the data support the hypothesis that nootkatone-induced toxicity is reasonably associated with a disruption in nitrogen nutrition – resulting in increased ammonium

uptake – several aspects of nootkatone's physiological impact remain to be fully elucidated. Chief among these is the identification of the primary factor driving the shift toward a predominantly ammonium-based nitrogen nutrition.

Nitrate assimilation is a highly energy-demanding process that requires both ATP and reducing equivalents. Under standard conditions, photorespiration plays a critical role in maintaining cellular redox balance by generating NADH in the mitochondria during glycine decarboxylation (Nunes-Nesi et al., 2010). It has been documented that inhibition of photorespiratory activity under high CO_2 results in a diminished capacity of the plants to reduce nitrate to ammonium, highlighting the critical role of photorespiration in maintaining redox balance and supporting nitrate reduction in C_3 plants (Bloom et al., 2010). Although further investigation is required, the observed decrease in glycolic acid levels with increasing concentrations of nootkatone in the growth medium (Fig. 3) points to a potential effect of this compound on the carboxylase/oxygenase activity of Rubisco. This, in turn, may indicate an involvement of the C_2 photorespiratory cycle in the reduced nitrate assimilation capacity observed in nootkatone-exposed plants. Moreover, a reduction in photorespiratory activity could also compromise the plant's ability to dissipate excess excitation energy generated during the light reactions of photosynthesis, thereby increasing susceptibility to photoinhibition (Kozaki and Takeba, 1996). This effect could further exacerbate the stress condition induced by ammonium accumulation in the green tissues. Within this conceptual framework, the overall availability of reducing power may potentially represent a key regulatory factor controlling the metabolic shift between nitrate and ammonium uptake. However, the limited amount of data currently available leaves room for alternative interpretations, in which the decrease in glycolate levels does not necessarily constitute evidence of lowered photorespiration. Instead, the decline in glycolate could plausibly reflect an accelerated turnover within the photorespiratory pathway, driven by enhanced transamination reactions and the high availability of amino donors. This interpretation is supported by the observed increase in photorespiratory amino acids – i.e., glycine and serine (Fig. 3) – which suggests that under nootkatone exposure, photorespiration operates in an "open" mode to provide carbon skeletons and detoxify excess ammonium. Such behavior has recently been observed in tomato leaves, where several photorespiratory enzyme activities (phosphoglycolate phosphatase, glycolate oxidase, hydroxypyruvate reductase) are maintained or even increased under ammonium stress, and serine synthesis is stimulated (Vega-Mas et al., 2024). In this way, the reduction in nitrate uptake observed in nootkatone-exposed plants could be interpreted as a consequence of redox and organic acid reallocation toward rapid ammonium assimilation, rather than as a necessary decline in Rubisco oxygenase activity or overall photorespiration. Further investigations will therefore be necessary to deepen and clarify the photorespiratory implications in the biological processes altered by nootkatone.

Finally, the fact that a single molecule can exert opposite effects on nitrate and ammonium uptake suggests that nootkatone may act on an upstream regulatory process controlling the preferential absorption of one nitrogen form over the other, possibly at the transcriptional level. However, it cannot be ruled out that the observed variations in nitrate and ammonium uptake are due to a direct interaction of nootkatone with the plasma membrane, nor that the reduction in nitrate uptake is simply the final outcome of enhanced ammonium uptake. In the latter scenario, the decrease in nitrate uptake could result from feedback regulation triggered by the accumulation of organic compounds containing reduced nitrogen (Orebamjo et al., 1975; Glass et al., 2002; Hachiya and Sakakibara, 2017; Rivero-Marcos, 2025). In all these contexts, the observed metabolic and physiological responses would result from altered nutritional preferences rather than from a direct, multifaceted effect of nootkatone on different processes.

Conclusions

This study provides a detailed mechanistic insight into the phytotoxicity of nootkatone in *Arabidopsis thaliana*. The integration of physiological, metabolic, and isotopic data supports the hypothesis that nootkatone interferes with primary metabolism and nitrogen nutrition by promoting ammonium over nitrate uptake. These alterations lead to metabolic imbalance and stress responses consistent with ammonium toxicity.

Given its natural origin and multifaceted bioactivity, nootkatone represents a promising candidate for the development of sustainable and environmentally friendly weed management strategies.

It should be noted that, although hydroponics provides precise control and high analytical reproducibility, it does not capture complex processes associated with soil dynamics (such as adsorption and degradation) or plant–soil–microbe interactions that may occur under field conditions, which could substantially influence nootkatone availability in natural environments. Moreover, the continuous exposure imposed by hydroponic systems may lead to an overestimation of nootkatone phytotoxicity compared with soil cultivation, where plants typically experience a single application followed by a gradual decline in compound concentration. Therefore, our findings should be interpreted within the context of a simplified system, and future soil-based studies using one-time application designs will be essential to assess the realistic relevance of nootkatone.

Importantly, based on the effects described in this study, we would also like to emphasize that nootkatone may serve as a valuable tool for dissecting the molecular mechanisms that regulate the preferential uptake of nitrate or ammonium when both nitrogen sources are available to plants.

CRediT authorship contribution statement

Alice Zambelli: Writing – review & editing, Investigation, Formal analysis, Data curation. **Michele Pesenti:** Writing – review & editing, Writing – original draft, Investigation, Formal analysis, Data curation. **Giorgio Lucchini:** Investigation, Formal analysis. **Adela María Sánchez-Moreiras:** Writing – review & editing. **Luca Espen:** Writing – review & editing, Investigation, Formal analysis. **Fabrizio Araniti:** Writing – review & editing, Writing – original draft, Investigation, Funding acquisition, Formal analysis, Data curation, Conceptualization. **Fabio Francesco Nocito:** Writing – review & editing, Writing – original draft, Investigation, Formal analysis, Data curation, Conceptualization.

Declaration of competing interest

The authors declare that they have no known competing financial interests or personal relationships that could have appeared to influence the work reported in this paper.

Acknowledgments

The European EU-Horizon project "AGROSUS: AGROecological strategies for SUStainable weed management in key European crop" funded the research under Grant Agreement Number 101084084.

Supplementary materials

Supplementary material associated with this article can be found, in the online version, at doi:10.1016/j.stress.2026.101223.

Data availability

Data will be made available on request.

References

Araniti, F., Graña, E., Reigosa, M.J., Sánchez-Moreiras, A.M., Abenavoli, M.R., 2013. Individual and joint activity of terpenoids, isolated from *Calamintha nepeta* extract, on *Arabidopsis thaliana*. Nat. Prod. Res. 27, 2297–2303. https://doi.org/10.1080/14786419.2013.827193.

Araniti, F., Graña, E., Krasuska, U., Bogatek, R., Reigosa, M.J., Abenavoli, M.R., Sanchez-Moreiras, A.M., 2016. Loss of gravitropism in farnesene-treated *Arabidopsis* is due to microtubule malformations related to hormonal and ROS unbalance. PloS One 11, e0160202. https://doi.org/10.1371/journal.pone.0160202.

Araniti, F., Bruno, L., Sunseri, F., Pacenza, M., Forgione, I., Bitonti, M.B., Abenavoli, M. R., 2017a. The allelochemical farnesene affects *Arabidopsis thaliana* root meristem altering auxin distribution. Plant Physiol. Biochem. 121, 14–20. https://doi.org/10.1016/j.plaphy.2017.10.005.

Araniti, F., Sánchez-Moreiras, A.M., Graña, E., Reigosa, M.J., Abenavoli, M.R., 2017b. Terpenoid *trans*-caryophyllene inhibits weed germination and induces plant water status alteration and oxidative damage in adult *Arabidopsis*. Plant Biol 19, 79–89. https://doi.org/10.1111/plb.12471.

Araniti, F., Landi, M., Lupini, A., Sunseri, F., Guidi, L., Abenavoli, M.R., 2018. *Origanum vulgare* essential oils inhibit glutamate and aspartate metabolism altering the photorespiratory pathway in *Arabidopsis thaliana* seedlings. J. Plant Physiol. 231, 297–309. https://doi.org/10.1016/j.jplph.2018.10.006.

Araniti, F., Miras-Moreno, B., Lucini, L., Landi, M., Abenavoli, M.R., 2020. Metabolomic, proteomic and physiological insights into the potential mode of action of thymol, a phytotoxic natural monoterpenoid phenol. Plant Physiol. Biochem. 153, 141–153. https://doi.org/10.1016/j.plaphy.2020.05.008.

Arora, S., Husain, T., Prasad, S.M., 2024. Allelochemicals as biocontrol agents: promising aspects, challenges and opportunities. S. Afr. J. Bot. 166, 503–511. https://doi.org/10.1016/j.sajb.2024.01.029.

Basu, S., Duren, W., Evans, C.R., Burant, C.F., Michailidis, G., Karnovsky, A., 2017. Sparse network modeling and metscape-based visualization methods for the analysis of large-scale metabolomics data. Bioinformatics 33, 1545–1553. https://doi.org/10.1093/bioinformatics/btx012.

Blacquière, T., Voortman, E., Stulen, I., 1988. Ammonium and nitrate nutrition in Plantago lanceolata L. and Plantago major L. ssp. Major: III. Nitrogen metabolism. Plant Soil. 106, 23–34. https://doi.org/10.1007/BF02371191.

Bloom, A.J., Burger, M., Asensio, J.S.R., Cousins, A.B., 2010. Carbon dioxide enrichment inhibits nitrate assimilation in wheat and arabidopsis. Science 328, 899–903. https://doi.org/10.1126/science.1186440.

Britto, D.T., Kronzucker, H.J., 2002. NH_4^+ toxicity in higher plants: a critical review. J. Plant Physiol. 159, 567–584. https://doi.org/10.1078/0176-1617-0774.

Britto, D.T., Kronzucker, H.J., 2005. Nitrogen acquisition, PEP carboxylase, and cellular pH homeostasis: new views on old paradigms. Plant Cell Environ 28, 1396–1409. https://doi.org/10.1111/j.1365-3040.2005.01372.x.

Buezo, J., Urra, M., González, E.M., Alcázar, R., Marino, D., Moran, J.F., 2025. The urea cycle in connection to polyamine metabolism in higher plants: new perspectives on a central pathway. Physiol. Plant. 177, e70321. https://doi.org/10.1111/ppl.70321.

Butnariu, M., Koirala, N., 2025. In: Policarpo Tonelli, F.M.P., Mushtaq, W., Roy, A., Öztürk, M., Policarpo Tonelli, F.C., Hakeem, K.R. (Eds.), Main Pathways Involved in the Production of Allelochemicals. Allelopathy. Apple Academic Press., New York, pp. 117–150.

Coleto, I., Marín-Peña, A.J., Urbano-Gámez, J.A., González-Hernández, A.I., Shi, W., Li, G., Marino, D., 2023. Interaction of ammonium nutrition with essential mineral cations. J. Exp. Bot. 74, 6131–6144. https://doi.org/10.1093/jxb/erad215.

Coskun, D., Britto, D.T., Li, M., Becker, A., Kronzucker, H.J., 2013. Rapid ammonia gas transport accounts for futile transmembrane cycling under NH_3/NH_4^+ toxicity in plant roots. Plant Physiol 163, 1859–1867. https://doi.org/10.1104/pp.113.225961.

Carillo, P., Cozzolino, C., D'Abrosca, B., Nacca, F., DellaGreca, M., Fiorentino, A., Fuggi, A., 2010. Effects of the allelochemicals dihydrodiconiferylalcohol and lariciresinol on metabolism of Lactuca sativa. Open Bioact. Compd. J. 3, 18–24. https://doi.org/10.2174/1874847301003010018.

Cataldo, D.A., Maroon, M., Schrader, L.E., Youngs, V.L., 1975. Rapid colorimetric determination of nitrate in plant tissue by nitration of salicylic acid. Commun. Soil Sci. Plant Anal. 6, 71–80. https://doi.org/10.1080/00103627509366547.

Chaimovitsh, D., Shachter, A., Abu-Abied, M., Rubin, B., Sadot, E., Dudai, N., 2017. Herbicidal activity of monoterpenes is associated with disruption of microtubule functionality and membrane integrity. Weed Sci 65, 19–30. https://doi.org/10.1614/WS-D-16-00044.1.

Chauhan, B.S., 2020. Grand challenges in weed management. Front. Agron. 1, 3. https://doi.org/10.3389/fagro.2019.00003.

Chen, Y., Zhang, L., Wang, J., 2011. Effects of coumarin application on plant growth and nitrogen metabolism in leaves of *Medicago sativa*. Allelopathy J 28, 105–114.

Clarkson, T.C., Janich, A.J., Sanchez-Vargas, I., Markle, E.D., Gray, M., Foster, J.R., Black IV, W.C., Foy, B.D., Olson, K.E., 2021. Nootkatone is an effective repellent against *Aedes aegypti* and *Aedes albopictus*. Insects 12, 386. https://doi.org/10.3390/insects12050386.

Dalal, V.K., Tripathy, B.C., 2018. Water-stress induced downsizing of light-harvesting antenna complex protects developing rice seedlings from photo-oxidative damage. Sci. Rep. 8, 5955. https://doi.org/10.1038/s41598-017-14419-4.

Davies, D.D., 1986. The fine control of cytosolic pH. Physiol. Plant. 67, 702–706. https://doi.org/10.1111/j.1399-3054.1986.tb05081.x.

Dayan, F.E., Duke, S.O., 2010. Natural products for weed management in organic farming in the USA. Outlooks Pest Manag 21, 156–160. https://doi.org/10.1564/21aug02.

Dietrich, G., Dolan, M.C., Peralta-Cruz, J., Schmidt, J., Piesman, J., Eisen, R.J., Karchesy, J.J., 2006. Repellent activity of fractioned compounds from *Chamaecyparis nootkatensis* essential oil against nymphal *Ixodes scapularis* (Acari: ixodidae). J. Medi. Entomol. 43, 957–961. https://doi.org/10.1093/jmedent/43.5.957.

Domínguez-Valdivia, M.D., Aparicio-Tejo, P.M., Lamsfus, C., Cruz, C., Martins-Loução, M.A., Moran, J.F., 2008. Nitrogen nutrition and antioxidant metabolism in ammonium-tolerant and sensitive plants. Physiol. Plant. 132, 359–369. https://doi.org/10.1111/j.1399-3054.2007.01022.x.

Du, W., Zhang, Y., Si, J., Zhang, Y., Fan, S., Xia, H., Kong, L., 2021. Nitrate alleviates ammonium toxicity in wheat (*Triticum aestivum* L.) by regulating tricarboxylic acid cycle and reducing rhizospheric acidification and oxidative damage. Plant Signal. Behav. 16, 1991687. https://doi.org/10.1080/15592324.2021.1991687.

Duke, S.O., Heap, I., 2017. Evolution of weed resistance to herbicides: what have we learned after 70 years? In: Jugulam, M. (Ed.), Biology, Physiology and Molecular Biology of Weeds. CRC Press., Boca Raton, pp. 63–86.

Duke, S.O., Pan, Z., Bajsa-Hirschel, J., Boyette, C.D., 2022. The potential future roles of natural compounds and microbial bioherbicides in weed management in crops. Adv. Weed Sci. 40 (Spec1), e020210054. https://doi.org/10.51694/AdvWeedSci/2022;40:seventy-five003.

Esteban, R., Ariz, I., Cruz, C., Moran, J.F., 2016. Review: mechanisms of ammonium toxicity and the quest for tolerance. Plant Sci 248, 92–101. https://doi.org/10.1016/j.plantsci.2016.04.008.

Fan, J., Liu, Z., Xu, S., Yan, X., Cheng, W., Yang, R., Guo, Y., 2022. Non-food bioactive product (+)-nootkatone: chemistry and biological activities. Ind. Crops Prod. 177, 114490. https://doi.org/10.1016/j.indcrop.2021.114490.

Ferri, A., Lancilli, C., Maghrebi, M., Lucchini, G., Sacchi, G.A., Nocito, F.F., 2017. The sulfate supply maximizing Arabidopsis shoot growth is higher under long- than short-term exposure to cadmium. Front. Plant Sci. 8, 854. https://doi.org/10.3389/fpls.2017.00854.

Forde, B.G., Lea, P.J., 2007. Glutamate in plants: metabolism, regulation, and signalling. J. Exp. Bot. 58, 2339–2358. https://doi.org/10.1093/jxb/erm121.

Glass, A.D.M., Britto, D.T., Kaiser, B.N., Kinghorn, J.R., Kronzucker, H.J., Kumar, A., Okamoto, M., Rawat, S., Siddiqi, M.Y., Unkles, S.E., Vidmar, J.J., 2002. The regulation of nitrate and ammonium transport systems in plants. J. Exp. Bot. 53, 855–864. https://doi.org/10.1093/jexbot/53.370.855.

Graña, E., Sotelo, T., Díaz-Tielas, C., Araniti, F., Krasuska, U., Bogatek, R., Reigosa, M.J., 2013. Citral induces auxin and ethylene-mediated malformations and arrests cell division in Arabidopsis thaliana roots. J. Chem. Ecol. 39, 271–282. https://doi.org/10.1007/s10886-013-0250-y.

Habash, S.S., Könen, P.P., Loeschcke, A., Wüst, M., Jaeger, K.-E., Drepper, T., Grundler, F.M.W., Schleker, A.S.S., 2020. The plant sesquiterpene nootkatone efficiently reduces Heterodera schachtii parasitism by activating plant defense. Int. J. Mol. Sci. 21, 9627. https://doi.org/10.3390/ijms21249627.

Hachiya, T., Inaba, J., Wakazaki, M., Sato, M., Toyooka, K., Miyagi, A., Kawai-Yamada, M., Sugiura, D., Nakagawa, T., Kiba, T., Gojon, A., Sakakibara, H., 2021. Excessive ammonium assimilation by plastidic glutamine synthetase causes ammonium toxicity in Arabidopsis thaliana. Nat. Commun. 12, 4944. https://doi.org/10.1038/s41467-021-25238-7.

Hachiya, T., Sakakibara, H., 2017. Interactions between nitrate and ammonium in their uptake, allocation, assimilation, and signaling in plants. J. Exp. Bot. 68, 2501–2512. https://doi.org/10.1093/jxb/erw449.

Harada, T., Takaki, H., Yamada, Y., 1968. Effect of nitrogen sources on the chemical components in young plants. Soil Sci. Plant Nutr. 14, 47–55. https://doi.org/10.1080/00380768.1968.10432008.

Hawkesford, M.J., Cakmak, I., Coskun, D., De Kok, L.J., Lambers, H., Schjoerring, J.K., White, P.J., 2023. Functions of macronutrients. In: Rengel, Z., Cakmak, I., White, P. J. (Eds.), Marschner's Mineral Nutrition of Plants, 4th Edition. Academic Press, San Diego, pp. 201–281.

Hejl, A.A., Einhellig, F.A., Rasmussen, J.A., 1993. Effects of juglone on growth, photosynthesis, and respiration. J. Chem. Ecol. 19, 559–568. https://doi.org/10.1007/BF00994325.

Hewitt, E.J., Gundry, C.S., 1970. The molybdenum requirement of plants in relation to nitrogen supply. J. Hortic. Sci. 45, 351–358. https://doi.org/10.1080/00221589.1970.11514364.

Hussain, M.I., González, L., Chiapusio, G., Reigosa, M.J., 2011. Benzoxazolin-2 (3H)-one (BOA) induced changes in leaf water relations, photosynthesis and carbon isotope discrimination in *Lactuca sativa*. Plant Physiol. Biochem. 49, 825–834. https://doi.org/10.1016/j.plaphy.2011.05.003.

Hussain, M.I., Reigosa, M.J., 2021. Secondary metabolites, ferulic acid and p-hydroxybenzoic acid induced toxic effects on photosynthetic process in *Rumex acetosa* L. Biomolecules 11, 233. https://doi.org/10.3390/biom11020233.

Kalcsits, L.A., Buschhaus, H.A., Guy, R.D., 2014. Nitrogen isotope discrimination as an integrated measure of nitrogen fluxes, assimilation and allocation in plants. Physiol. Plantarum 151, 293–304. https://doi.org/10.1111/ppl.12167.

Kozaki, A., Takeba, G., 1996. Photorespiration protects C3 plants from photooxidation. Nature 384, 557–560. https://doi.org/10.1038/384557a0.

Landi, M., Misra, B.B., Muto, A., Bruno, L., Araniti, F., 2020. Phytotoxicity, morphological, and metabolic effects of the sesquiterpenoid nerolidol on *Arabidopsis thaliana* seedling roots. Plants 9, 1347. https://doi.org/10.3390/plants9101347.

Leonhardt, R.H., Berger, R.G., 2015. Nootkatone. In: Schrader, J., Bohlmann, J. (Eds.), Biotechnology of Isoprenoids. Springer Cham., Hannover, pp. 391–404.

Li, G., Wang, Z., Zhang, L., Kronzucker, H.J., Chen, G., Wang, Y., Shi, W., Li, Y., 2025. The role of the nitrate transporter NRT1.1 in plant iron homeostasis and toxicity on ammonium. Environ. Exp. Bot. 232, 106112. https://doi.org/10.1016/j.envexpbot.2025.106112.

López-González, D., Costas-Gil, A., Reigosa, M.J., Araniti, F., Sánchez-Moreiras, A.M., 2020. A natural indole alkaloid, norharmane, affects PIN expression patterns and compromises root growth in *Arabidopsis thaliana*. Plant Physiol. Biochem. 151, 378–390. https://doi.org/10.1016/j.plaphy.2020.03.047.

Lupini, A., Araniti, F., Mauceri, A., Princi, M.P., Sorgonà, A., Sunseri, F., Varanini, Z., Abenavoli, M.R., 2018. Coumarin enhances nitrate uptake in maize roots through modulation of plasma membrane H^+-ATP ase activity. Plant Biol 20, 390–398. https://doi.org/10.1111/plb.12674.

Macías, F.A., Marín, D., Oliveros-Bastidas, A., Simonet, A.M., Molinillo, J.M., 2022. In: Fujii, Y., Hiradate, Y. (Eds.), Ecological Relevance of the Degradation Processes of Allelochemicals. Allelopathy. CRC Press., Boca Raton, pp. 91–107.

Magalhaes, J.R., Wilcox, G.E., 1984. Growth, free amino acids, and mineral composition of tomato plants in relation to nitrogen form and growing media. J. Am. Soc. Hortic. Sci. 109, 406–411. https://doi.org/10.21273/JASHS.109.3.406.

Majerowicz, N., Kerbauy, G.B., Nievola, C.C., Suzuki, R.M., 2000. Growth and nitrogen metabolism of *catasetum fimbriatum* (orchidaceae) grown with different nitrogen sources. Environ. Exp. Bot. 44, 195–206. https://doi.org/10.1016/S0098-8472(00)00066-6.

Mao, L., Henderson, G., Laine, R.A., 2004. Germination of various weed species in response to vetiver oil and nootkatone. Weed Technol. 18, 263–267. https://doi.org/10.1614/WT-03-034R2.

Mao, L., Henderson, G., Bourgeois, W.J., Vaughn, J.A., Laine, R.A., 2006. Vetiver oil and nootkatone effects on the growth of pea and citrus. Ind. Crops Prod. 23, 327–332. https://doi.org/10.1016/j.indcrop.2005.09.004.

M'barek, K., 2016. Chemical composition and phytotoxicity of *Cupressus sempervirens* leaves against crops. J. Essent. Oil-Bear. Plants 19, 1582–1599. https://doi.org/10.1080/0972060X.2016.1226964.

Mendel, R.R., Hänsch, R., 2002. Molybdoenzymes and molybdenum cofactor in plants. J. Exp. Bot. 53, 1689–1698. https://doi.org/10.1093/jxb/erf038.

Misra, B., 2019. Steps for building an open source EI-MS mass spectral library for GC–MS-based metabolomics. Metabolom. Protocol. Workflow. https://doi.org/10.17504/protocols.io.8txhwpn.

Misra, B.B., Das, V., Landi, M., Abenavoli, M.R., Araniti, F., 2020. Short-term effects of the allelochemical umbelliferone on *Triticum durum* L. metabolism through GC–MS based untargeted metabolomics. Plant Sci 298, 110548. https://doi.org/10.1016/j.plantsci.2020.110548.

Nunes-Nesi, A., Fernie, A.R., Stitt, M., 2010. Metabolic and signaling aspects underpinning the regulation of plant carbon nitrogen interactions. Mol. Plant 3, 973–996. https://doi.org/10.1093/mp/ssq049.

Orasen, G., De Nisi, P., Lucchini, G., Abruzzese, A., Pesenti, M., Maghrebi, M., Kumar, A., Nocito, F.F., Baldoni, E., Morgutti, S., Negrini, N., Valè, G., Sacchi, G.A., 2019. Continuous flooding or alternate wetting and drying differently affect the accumulation of health-promoting phytochemicals and minerals in rice brown grain. Agronomy 9, 628. https://doi.org/10.3390/agronomy9100628.

Orebamjo, T.O., Stewart, G.R., 1975. Ammonium repression of nitrate reductase formation in *Lemna minor* L. Planta 122, 27–36. https://doi.org/10.1007/BF00385401.

Palanivel, H., Tilaye, G., Belliathan, S.K., Benor, S., Abera, S., Kamaraj, M., 2021. Allelochemicals as natural herbicides for sustainable agriculture to promote a cleaner environment. In: Aravind, J., Kamaraj, M., Prashanthi Devi, M., Rajakumar, S. (Eds.), Strategies and Tools for Pollutant Mitigation: Avenues to a Cleaner Environment. Springer Cham., Hannover, pp. 93–166.

Panella, N.A., Dolan, M.C., Karchesy, J.J., Xiong, Y., Peralta-Cruz, J., Khasawneh, M., Montenieri, J.A., Maupin, G.O., 2005. Use of novel compounds for pest control: insecticidal and acaricidal activity of essential oil components from heartwood of Alaska yellow cedar. J. Med. Entomol. 42, 352–358. https://doi.org/10.1093/jmedent/42.3.352.

Pang, Z., Lu, Y., Zhou, G., Hui, F., Xu, L., Viau, C., Spigelman, A.F., MacDonald, P.E., Wishart, D.S., Li, S., Xia, J., 2024. MetaboAnalyst 6.0: towards a unified platform for metabolomics data processing, analysis and interpretation. Nucleic Acids Res 52, W398–W406. https://doi.org/10.1093/nar/gkae253.

Powles, S.B., Yu, Q., 2010. Evolution in action: plants resistant to herbicides. Ann. Rev. Plant Biol. 61, 317–347. https://doi.org/10.1146/annurev-arplant-042809-112119.

Prinsi, B., Espen, L., 2018. Time-course of metabolic and proteomic responses to different nitrate/ammonium availability in roots and leaves of maize. Int. J. Mol. Sci. 19, 2202. https://doi.org/10.3390/ijms19082202.

Rastegar, S., Sayyad-Amin, P., 2025. GABA and oxidative stress and the regulation of antioxidants. In: Singh, S., Tripathi, D.K., Singh, V.P. (Eds.), GABA in Plants. John Wiley & Sons, Ltd., Chichester, pp. 225–241.

Rivero-Marcos, M., 2025. Functional crosstalk between nitrate and ammonium transporters in N acquisition and pH homeostasis. Front. Plant Sci. 16, 1634119. https://doi.org/10.3389/fpls.2025.1634119.

Salsac, L., Chaillou, S.S., Morot-Gaudry, J.F., Lesaint, C., Jolivet, E., 1987. Nitrate and ammonium nutrition in plants. Plant Physiol. Biochem. 25, 805–812.

Satyanarayana Murthy, I., Jolly, G.E., John, A.P., 2025. Allelopathy in weed management: a comprehensive review. Int. J. Plant & Soil Sci. 37, 96–104. https://doi.org/10.9734/ijpss/2025/v37i55434.

Sumner, L.W., Amberg, A., Barrett, D., Beale, M.H., Beger, R., Daykin, C.A., Fan, T.W., Fiehn, O., Goodacre, R., Griffin, J.L., Hankemeier, T., Hardy, N., Harnly, J., Higashi, R., Kopka, J., Lane, A.N., Lindon, J.C., Marriott, P., Nicholls, A.W., Reily, M.D., Thaden, J.J., Viant, M.R., 2007. Proposed minimum reporting standards for chemical analysis: chemical Analysis Working Group (CAWG) Metabolomics Standards Initiative (MSI). Metabolomics 3, 211–221. https://doi.org/10.1007/s11306-007-0082-2.

Uddin, M.R., Park, K.W., Han, S.M., Pyon, J.Y., Park, S.U., 2012. Effects of sorgoleone allelochemical on chlorophyll fluorescence and growth inhibition in weeds. Allelopathy J 30, 61–70.

Urra, M., Buezo, J., Royo, B., Cornejo, A., López-Gómez, P., Cerdán, D., Esteban, R., Martínez-Merino, V., Gogorcena, Y., Tavladoraki, P., Moran, J.F., 2022. The importance of the urea cycle and its relationships to polyamine metabolism during ammonium stress in *Medicago truncatula*. J. Exp. Bot. 73, 5581–5595. https://doi.org/10.1093/jxb/erac235.

Van Beusichem, M.L., Kirkby, E.A., Baas, R., 1988. Influence of nitrate and ammonium nutrition on the uptake, assimilation, and distribution of nutrients in *Ricinus communis*. Plant Physiol 86, 914–921. https://doi.org/10.1104/pp.86.3.914.

Vega-Mas, I., Marino, D., De la Peña, M., Fuertes-Mendizábal, T., González-Murua, C., Estavillo, J.M., González-Moro, M.B., 2024. Enhanced photorespiratory and TCA pathways by elevated CO_2 to manage ammonium nutrition in tomato leaves. Plant Physiol. Biochem. Volume 217, 109216. https://doi.org/10.1016/j.plaphy.2024.109216.

Verdeguer, M., Sánchez-Moreiras, A.M., Araniti, F., 2020. Phytotoxic effects and mechanism of action of essential oils and terpenoids. Plants 9, 1571. https://doi.org/10.3390/plants9111571.

Wang, Y.B., Li, J.L., Xu, F.F., Han, X.D., Wu, Y.S., Liu, B., 2022. (+)-Nootkatone: progresses in synthesis, structural modifications, pharmacology and ecology uses. Cur. Chin. Sci. 2, 129–142. https://doi.org/10.2174/2210298102666220117141156.

Wdowiak, A., Kryzheuskaya, K., Podgórska, A., Paterczyk, B., Zebrowski, J., Archacki, R., Szal, B., 2024. Ammonium nutrition modifies cellular calcium distribution influencing ammonium-induced growth inhibition. J. Plant Physiol. 298, 154264. https://doi.org/10.1016/j.jplph.2024.154264.

Westwood, J.H., Charudattan, R., Duke, S.O., Fennimore, S.A., Marrone, P., Slaughter, D.C., Swanton, C., Zollinger, R., 2018. Weed management in 2050: perspectives on the future of weed science. Weed Sci 66, 275–285. https://www.jstor.org/stable/26505840.

Widhalm, J.R., Dudareva, N., 2015. A familiar ring to it: biosynthesis of plant benzoic acids. Mol. Plant 8, 83–97. https://doi.org/10.1016/j.molp.2014.12.001.

Xiao, C., Fang, Y., Wang, S., He, K., 2023. The alleviation of ammonium toxicity in plants. *J. Integr.* Plant Biol. 65, 1362–1368. https://doi.org/10.1111/jipb.13467.

Yu, L., Zhao, H., Chen, G., Yuan, S., Lan, T., Zeng, J., 2020. Allelochemical-driven N preference switch from NO3− to NH4+ affecting plant growth of *Cunninghamia lanceolata* (lamb.) hook. Plant Soil 451, 419–434. https://doi.org/10.1007/s11104-020-04539-8.

Zambelli, A., Nocito, F.F., Araniti, F., 2025. Unveiling the multifaceted roles of root exudates: chemical interactions, allelopathy, and agricultural applications. Agronomy 15, 845. https://doi.org/10.3390/agronomy15040845.

Zhang, L.L., Chen, Y., Li, Z.J., Fan, G., Li, X., 2022. Production, function, and applications of the sesquiterpenes valencene and nootkatone: a comprehensive review. J. Agric. Food Chem. 71, 121–142. https://doi.org/10.1021/acs.jafc.2c07543.

Zhou, X., Song, H., Wang, J., 2013. Effects of coumarin on net nitrate uptake and nitrogen metabolism in roots of alfalfa (*Medicago sativa*). Allelopathy J 31, 377–386.